S11 Measurements Before and During the EDGES Deployment of October 2014

Raul Monsalve

SESE, Arizona State University

November 5, 2014

Description

This report describes the relevant steps followed to derive the calibration quantities needed to conduct S_{11} measurements at the input of the EDGES receiver. It also describes tests conducted at the MRO, as well as the antenna measurements performed the last days of the deployment. To make things easier to understand, the material is presented slide by slide.

Figure 1

The next slide (Figure 1) presents a diagram that summarizes the steps needed to obtain a calibrated S_{11} measurement at the receiver input. First, switch #1 routes the antenna to the VNA path by providing 12V to its power input (with 0V, the switch chooses the LNA route). With the VNA path selected, the VNA starts measuring the four devices connected to switch #2. Three of them correspond to transference reflection standards, in green: an open, short, and match. The fourth position measures the antenna or any device connected to the receiver input, in series with the switch paths.

At this point, the reference plane is around switch #2 where the transference standards are. However, we need to shift this plane to the input connector. The difference between the two planes is modeled as a block with S-parameters. Port 1 of this block faces the plane established by the transference standards, and Port 2 is at the input connector. If the S-parameters of this block were known, the calibrated measurement relative to the transference plane (Γ_{P1}) could be related to the value at the input (Γ_{P2}), by

$$\Gamma_{P1} = S_{11} + \frac{S_{12}S_{21} \cdot \Gamma_{P2}}{1 - S_{22} \cdot \Gamma_{P2}}, \tag{1}$$

and thus, the reflection at the input can be obtained by solving for Γ_{P2},

$$\Gamma_{P2} = \frac{\Gamma_{P1} - S_{11}}{S_{12}S_{21} + S_{22} \cdot (\Gamma_{P1} - S_{11})}. \tag{2}$$

The S-parameters of the block are obtained by measuring well known open, short, and match standards at the input connector, instead of the antenna. The measurements of these standards are calibrated at the transference plane, and then compared to their assumed true values. The S-parameters are then computed using

$$\begin{bmatrix} S_{11} \\ S_{12}S_{21} - S_{11}S_{22} \\ S_{22} \end{bmatrix} = \begin{bmatrix} 1 & \Gamma_o & \Gamma_o \cdot \Gamma'_o \\ 1 & \Gamma_s & \Gamma_s \cdot \Gamma'_s \\ 1 & \Gamma_m & \Gamma_m \cdot \Gamma'_m \end{bmatrix}^{-1} \begin{bmatrix} \Gamma'_o \\ \Gamma'_s \\ \Gamma'_m \end{bmatrix}. \tag{3}$$

where Γ_o, Γ_s, and Γ_m, are the true values of the standards, and Γ'_o, Γ'_s, and Γ'_m are their measurements at the transference plane.

A final important aspect to mention is that this characterization is valid at a specific temperature. Therefore, corrections have to be applied when the reference temperature differs from the one used for the fiducial characterization.

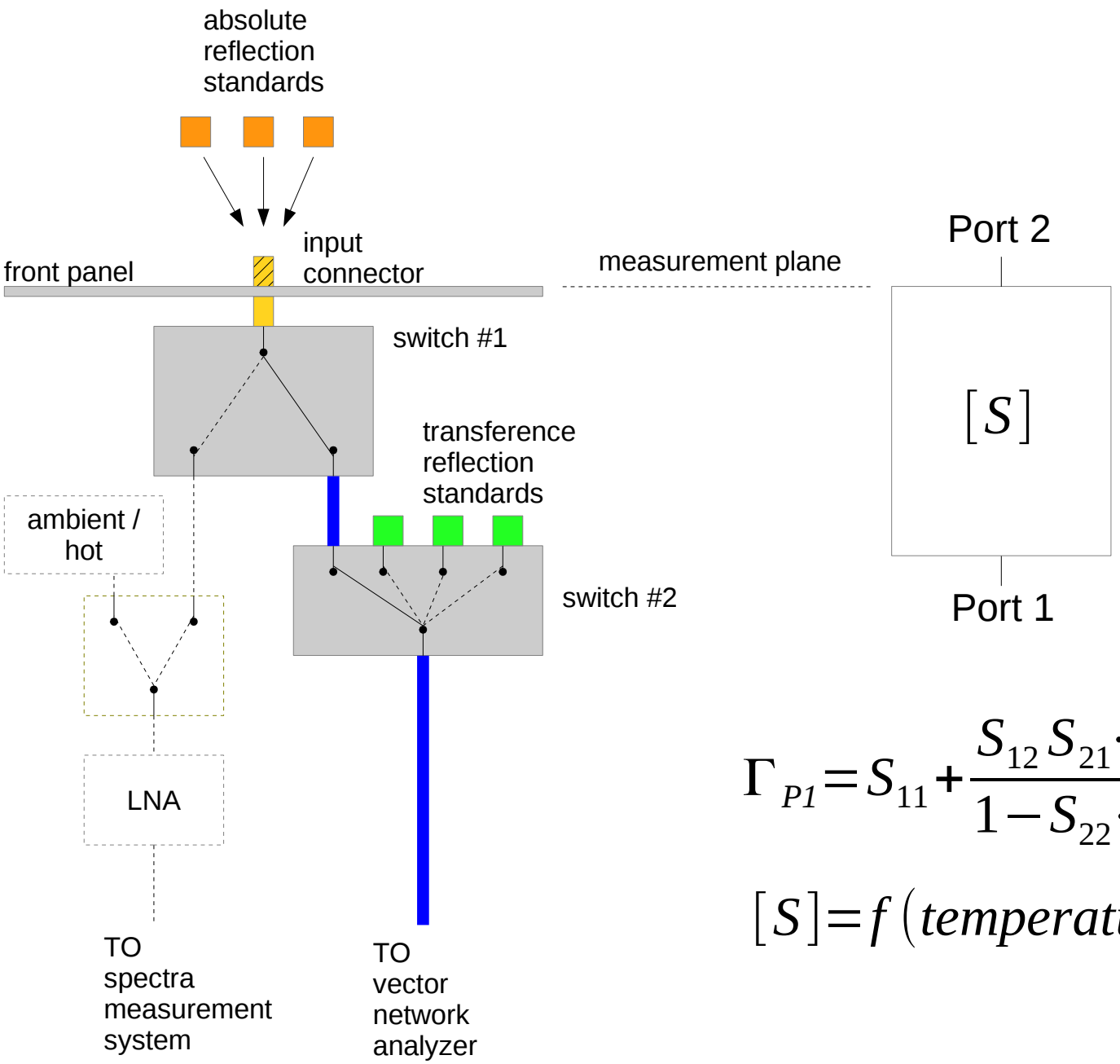

$$\Gamma_{P1} = S_{11} + \frac{S_{12} S_{21} \cdot \Gamma_{P2}}{1 - S_{22} \cdot \Gamma_{P2}}$$

$$[S] = f(temperature)$$

Figure: (1) Diagram of the S_{11} measurement setup.

Figure 2

The next slide (Figure 2) shows the S-parameters of the block described previously, which provide calibrated reflection measurements at the input connector.

Here is a list of relevant details regarding the computation of these S-parameters:

1. The standards measured at the input connector belong to the calkit Agilent 85033E.
2. The actual DC resistance of the match standard was used to model it, instead of the assumed 50 Ω.
3. A delay of 0 ps was assumed for the match standard.
4. The relevant settings of the Fieldfox VNA were: frequency range 50-200 MHz, resolution 1 MHz, IF bandwidth 300 Hz, power level 5dB, no average performed by the instrument itself (but see below).
5. Each standard (open, short, match) was measured continuously for approximately 12 hours, with the system in thermal equilibrium for most of the measurement. Since each measurement cycle (corresponding to the measurement of the three transference standards, and the standard at the input) takes 1 minute almost exactly, there are about 750 measurements calibrated at the transference plane for each absolute standard.
6. The reference temperature (measured with a fixed thermistor attached next to switch #2) was $27.4 \pm 0.2^\circ$C during the measurement of the three absolute standards. This temperature was reached in 50 minutes or less (coming up from $\sim 25^\circ$C, established by the closed-loop temperature control), after which it stayed stable to within 0.2°C.
7. With all the above, the S-parameters shown in Figure 2 were obtained:
   - calibrating all the measurements at the transference plane,
   - for each absolute standard, averaging the measurements taken after 50 minutes (leaving a total of $\sim$ 700 useful measurements) in order to minimize noise,
   - and using equation (3), with Γ_x representing the model of the standards and Γ'_x representing their averaged measurements.
8. These parameters are valid at $27.4 \pm 0.2^\circ$C. This is the temperature to which switch #2 arrives after 50 minutes of operation when the temperature controller keeps the LNA at 25°C, and ambient temperature is $\sim 23^\circ$C. When the temperature of switch #2 departs from this fiducial temperature (for example, due to higher ambient temperature), an extra correction is applied, described next.

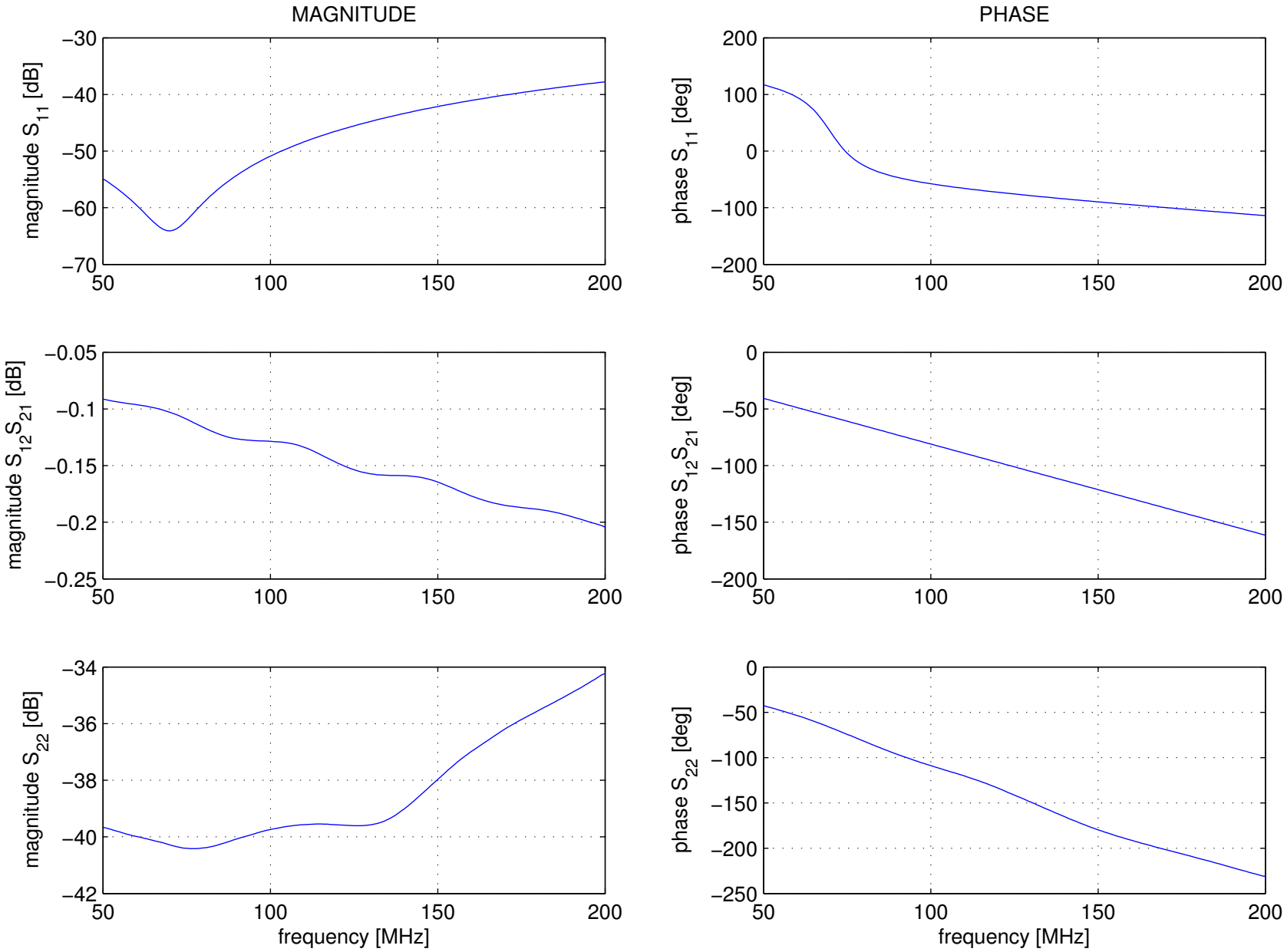

Figure: (2) Fiducial S-parameters that shift the reflection measurement plane to the input connector. They are valid when the temperature at switch #2 is 27.4±0.2°C. If this is not the case, a small correction is applied.

Figure 3

The reference temperature is measured in each cycle, along with the reflection of the transference standards. A correction has to be applied to the reflection of the device at the input connector (calibrated at the transference plane) based on the departure of the reference temperature from its fiducial value of 27.4°C. Variations with temperature of the real and imaginary parts of these complex quantities are smooth, and were modeled with 2nd degree polynomials.

The performance of this correction was tested by measuring devices at the input connector, with changing reference temperature. Specifically, the next slide (Figure 3) shows the measurement of a 50-Ω termination subject to a quite stable ambient temperature ($\sim$ 23.4°C), while the reference temperature of switch #2 was varying. The corrected measurement consistently shows the expected value (-58.72 dB, for a measured DC resistance of 50.116 Ω).

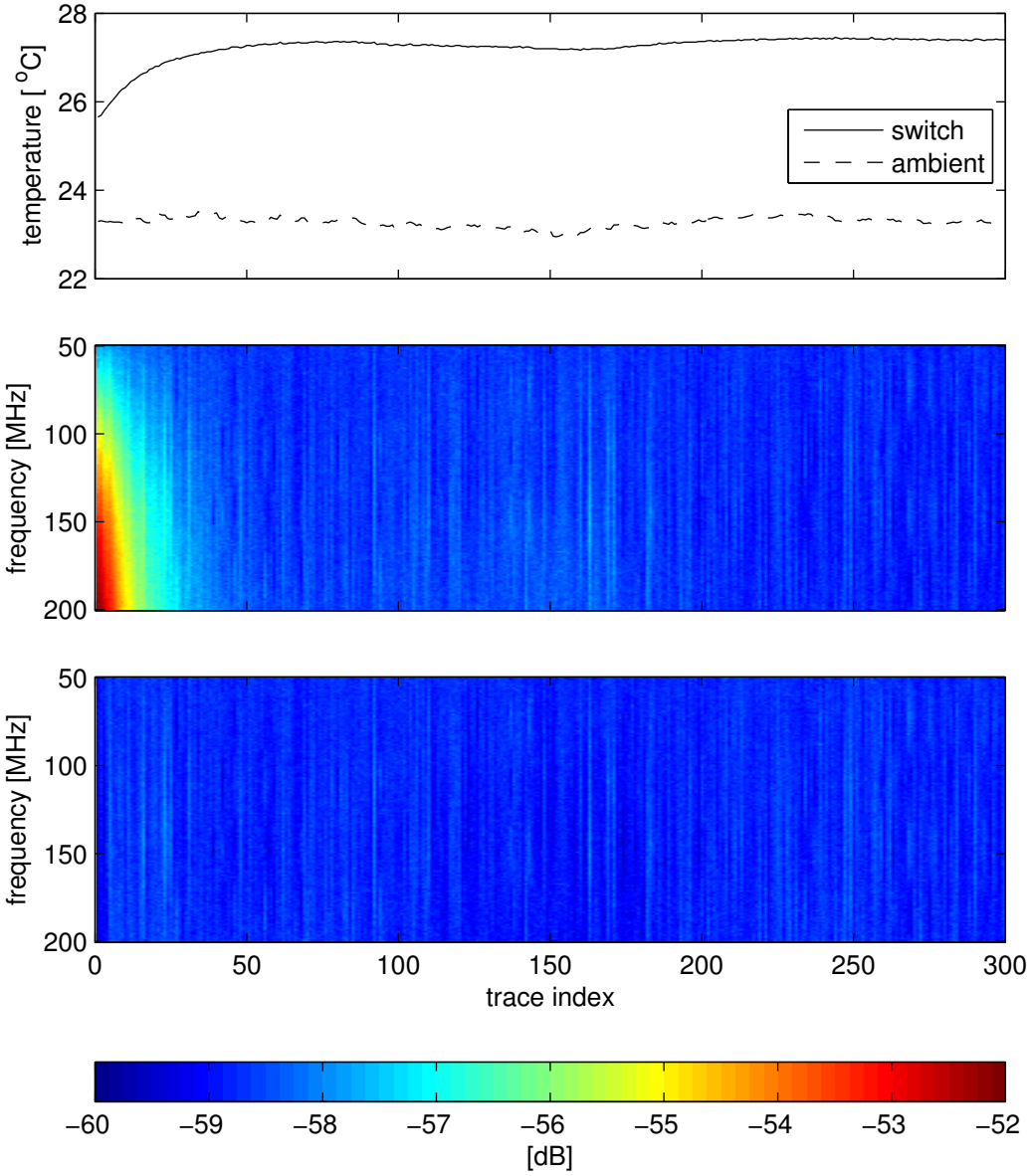

Figure: (3) Test of temperature correction for a 50-Ω termination (actual DC resistance of 50.116 Ω, corresponding to -58.72 dB). The device was subject to ambient temperature ($\sim$ 23.4°C), while the switch temperature was varying from $\sim$ 25.6°C to $\sim$ 27.4°C, which produced a varying reflection (middle panel). After applying the correction due to temperature changes, the reflection meets the expectations (lower panel). The residual fluctuations correspond primarily to instrument noise for such low reflections.

Figures 4 and 5

Two more tests conducted in the lab correspond to the comparison of the reflection delivered by this system using the Fieldfox VNA, after applying the corrections, with the reflection reported by the lab VNA Agilent E5072A with the measurement performed directly at its input port. This is an interesting comparison since the E5072A is more stable and less noisy, and also we are bypassing all the switching hardware (and associated assumptions and corrections), and therefore the measurement with the E5072A reflection should not be affected by that many systematic effects.

The test loads corresponded to an open-ended 6-dB attenuator, and an open-ended 25-ft cable. They were measured for one hour at the input of the receiver, and then their calibrated responses were averaged offline. The measurements done with the E5072A correspond to the average of 999 traces performed internally by this VNA.

The difference between measurements at the input of the receiver with the Fieldfox VNA, and at the input of the E5072A VNA, are of order 0.01 dB in magnitude and 0.05° in phase for the attenuator, and 0.015 dB in magnitude and 0.07° in phase for the cable. As expected, the structure of the differences vary, but it is ripply in general. For the attenuator, the result with the E5072A is much flatter and, thus, it is believed to represent reality better. Also, for the attenuator, a measurement of its DC resistance helps confirm that neither reflection measurement is farther than about 0.01 dB from the true value.

These comparisons are presented in Figures 4 and 5.

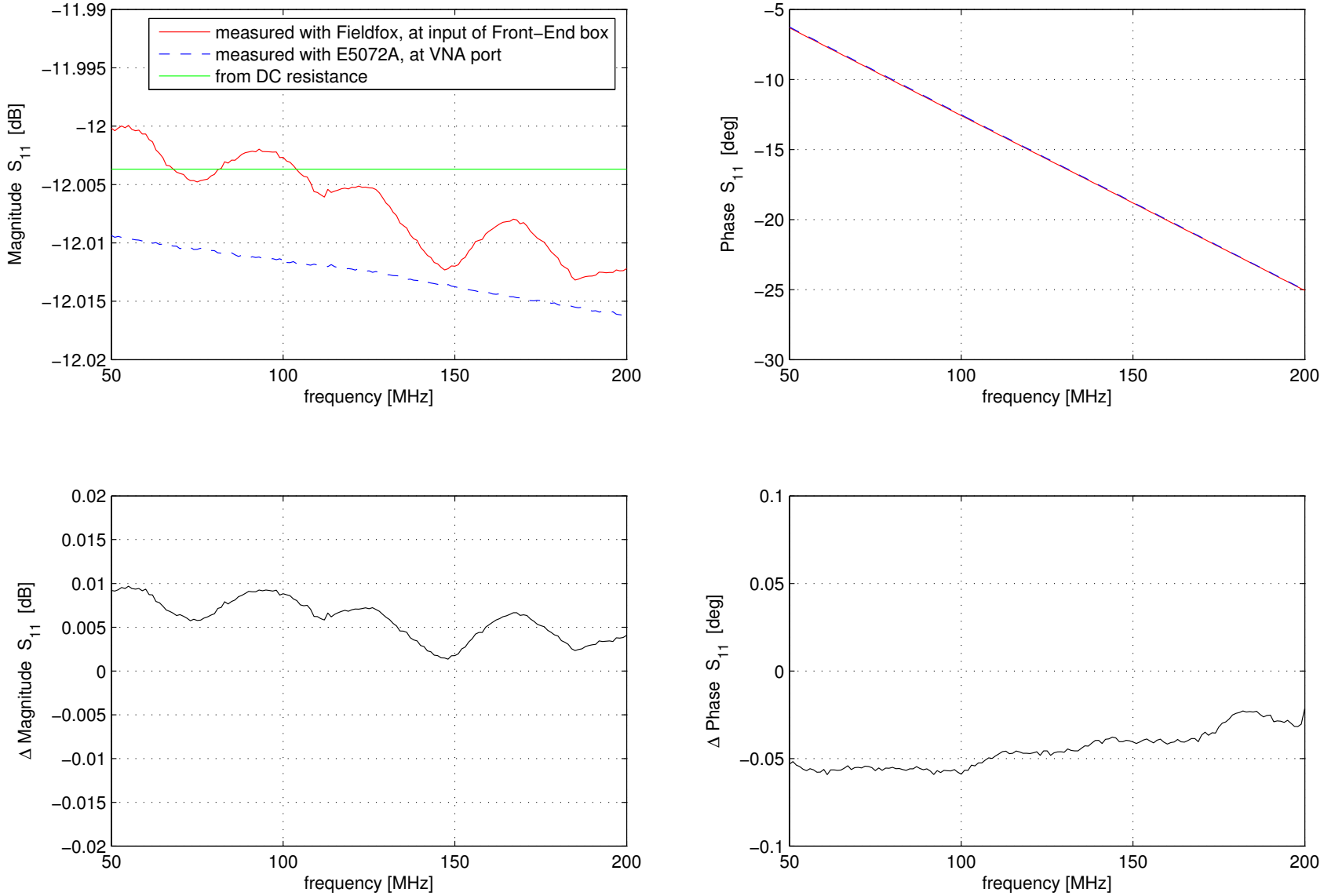

Figure: (4) Measurements of an open-ended 6-dB attenuator with the system incorporated into the EDGES receiver, which includes a Fieldfox VNA, and also at the input of an Agilent E5072A VNA. The reflection magnitude derived from the DC resistance of the attenuator is also shown. The differences between measurements are of order 0.01 dB in magnitude and 0.05° in phase.

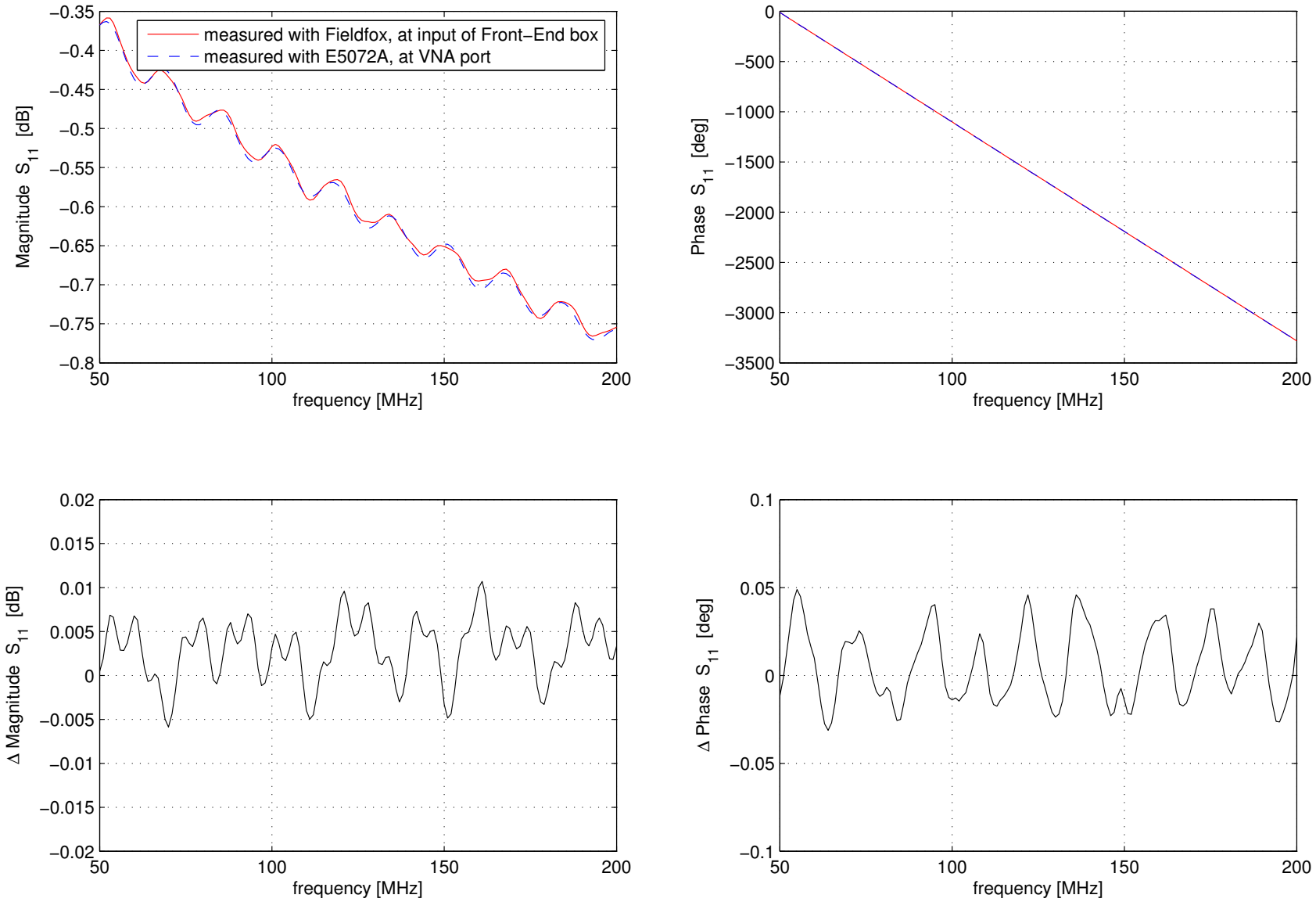

Figure: (5) Measurements of an open-ended 25-ft cable with the system incorporated into the EDGES receiver, which includes a Fieldfox VNA, and also at the input of an Agilent E5072A VNA. The peak-to-peak differences between measurements are about 0.015 dB in magnitude and 0.07° in phase.

Figures 6, 7, and 8

Once at the MRO, the reflection measurement system was tested using an open-ended 7-dB attenuator. The purpose of this test was to confirm that the performance of the system remained as expected, by measuring a device that provided a reflection that could be modeled by a line, and then analyzing the residuals. The results are presented in Figures 6, 7, and 8.

Figure 6 shows the residuals after removing a line from the magnitude and phase from the first measurements of the attenuator. The top panels show the residuals for the average of 4 measurements. They look as expected, with the residuals having reasonable amplitudes. On the other hand, the bottom panels show the residuals for a single measurement, also taken during preliminary runs, which obviously show large ripples. The appearance of these ripples demanded a longer term monitoring of the attenuator, and therefore a 3.25-hour long measurement was conducted.

Figure 7 shows the response of the transference open and short during this measurement. Obviously, the main feature of these data sets is the development of ripples with a period (in the frequency domain) of almost 20 MHz. These ripples are always evolving and, therefore, if they change faster than the duration of the reflection measurement cycles, residual ripples will propagate to the load being measured at the receiver input. However, out of the $\sim$ 190 traces obtained, only about 9 show significant ripples above the noise, corresponding to 5%. Therefore, it can be concluded that for the most part the calibration speed is appropriate, but it will be necessary to examine the antenna data so traces with ripples can be discarded from the analyses. Although it is difficult to prove, rapid changes in the setup could be attributed to the very long cable used in the field (115 meters) being subject to significant temperature changes. This was not a factor during tests in the lab, where a much shorter cable was used and temperature was well regulated.

Figure 8 shows average measurements of the attenuator obtained during the $\sim$ 3-hour measurement. Since during this test the receiver and base plate were mounted on sawhorses above ground, the attenuator was exposed to changes in ambient temperature and therefore the first and last 25-trace averages shown in the figure evidence a change in magnitude. The black traces correspond to the average of all the measurements (except the 5% with ripples), which means that the residuals observed are not dominated by noise, but instead represent systematic effects that this setup does not account for. However, despite having been measured in the field under much less stable conditions, the level of residuals is the same as that observed in the lab (Figures 4 and 5).

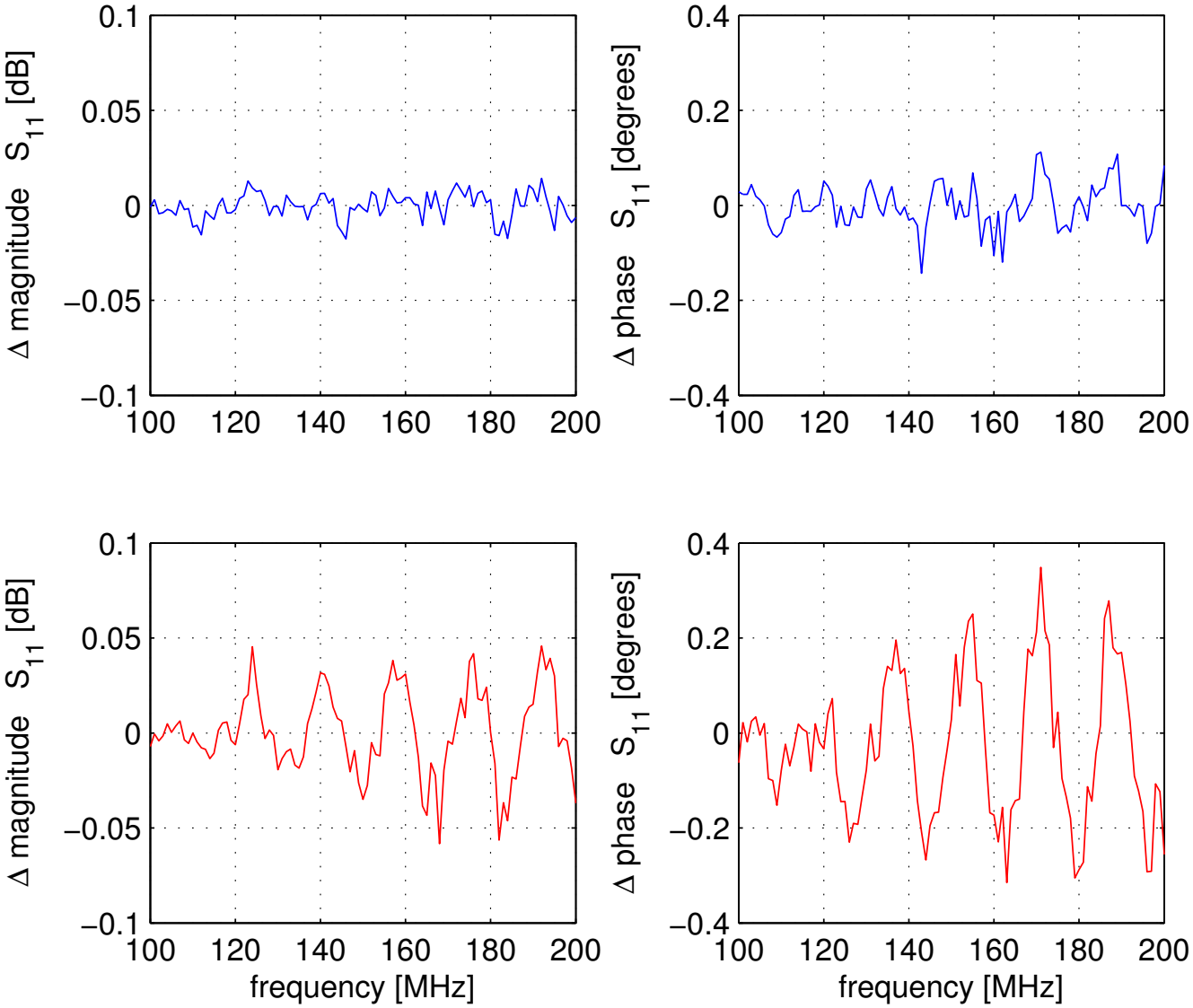

Figure: (6) Residuals from linear fits to the magnitude and phase of a 7-dB attenuator, conducted at the MRO. TOP: Residuals for the average of 4 normal measurements. BOTTOM: Residuals for a measurement that shows significant ripples. The appearance of large ripples in these measurements is an exception.

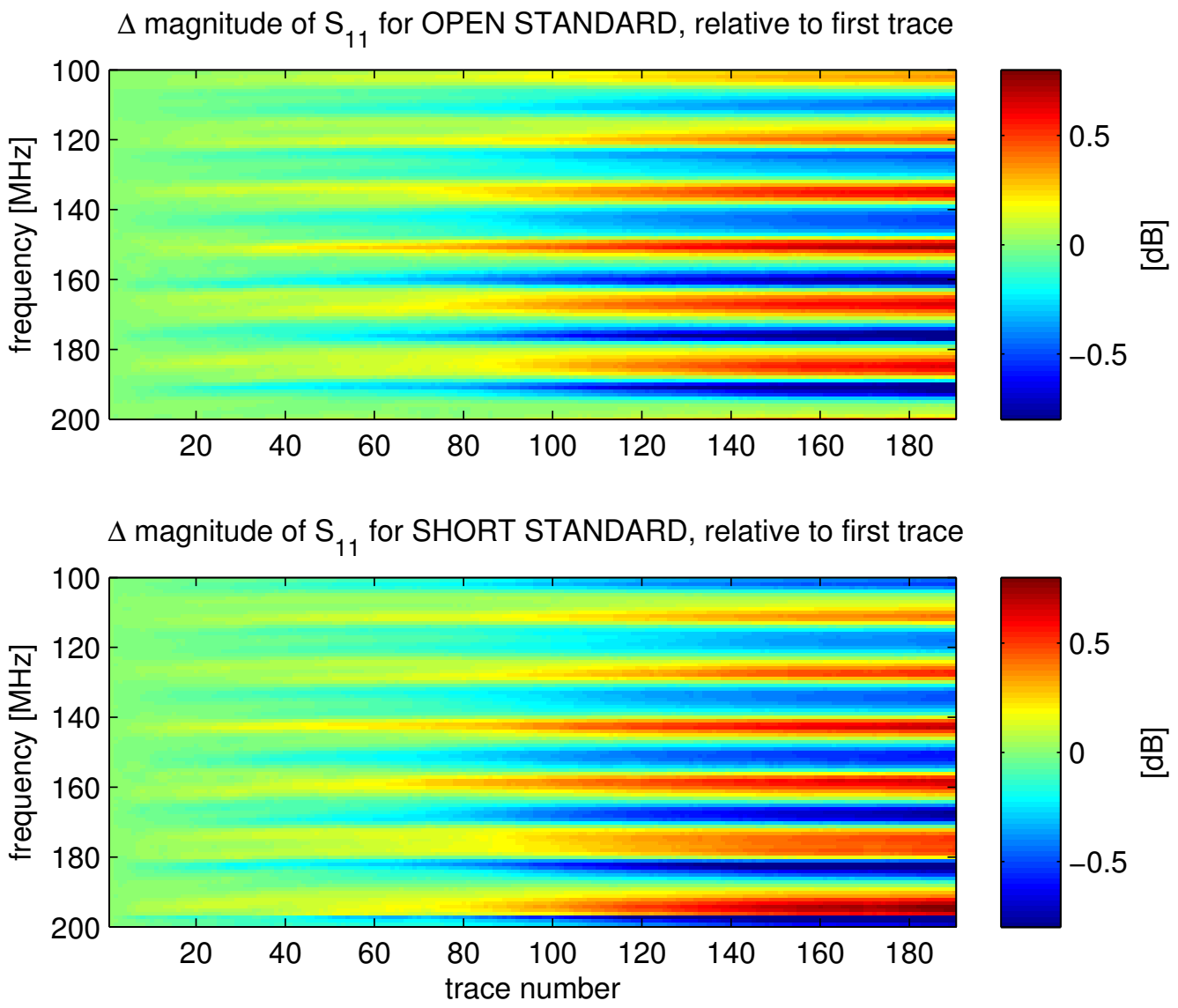

Figure: (7) Ripples are constantly being developed in the measurement setup, as evidenced in the data of the open and short transference standards, measured in parallel to the 7-dB attenuator. If these changes are fast, the calibration routine will not be able of calibrating them away. Fortunately, for the majority of measurements the drifts can be calibrated away, so the traces of the device under test are not affected by significant ripples.

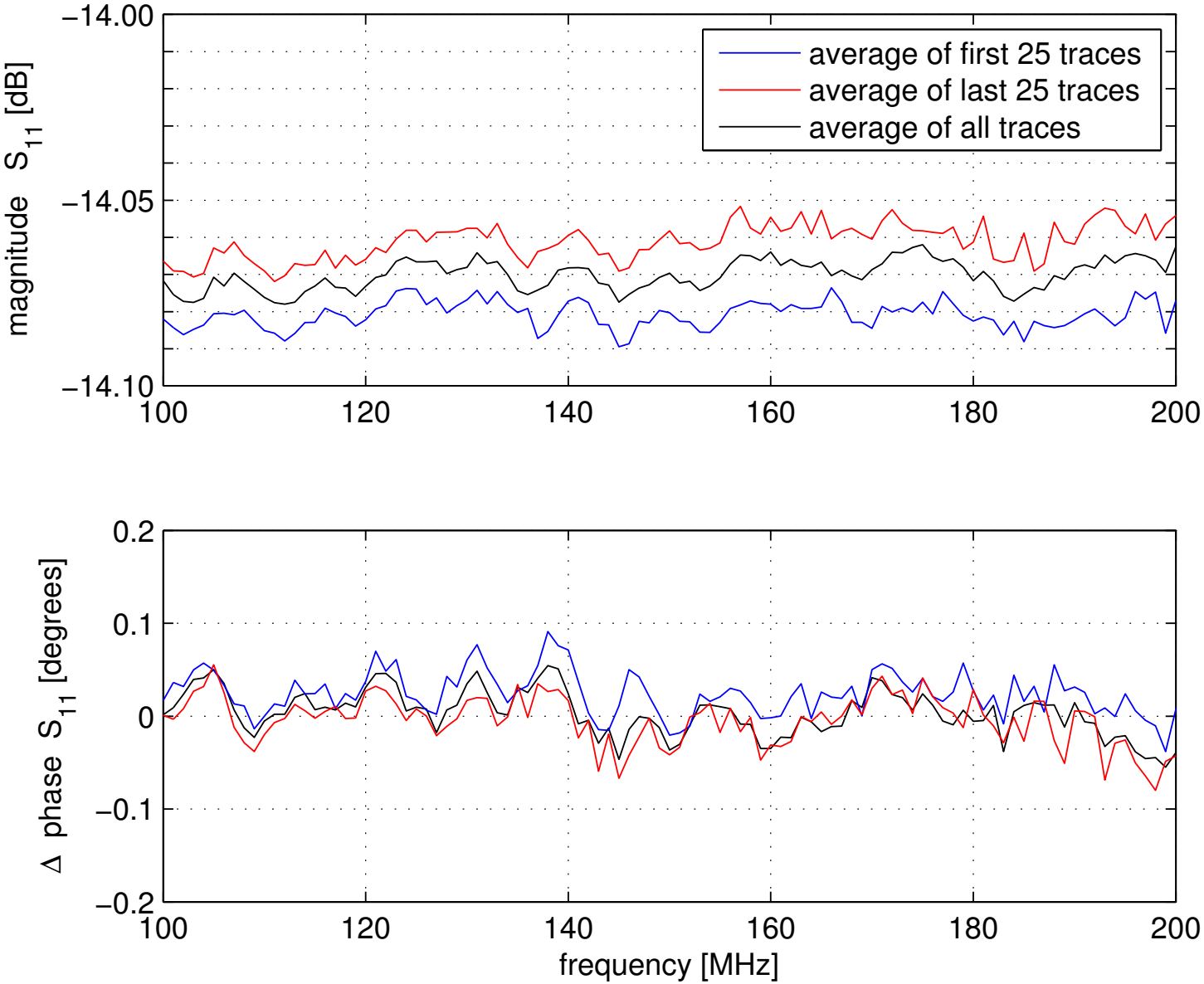

Figure: (8) Average of attenuator measurements (for the phase, a linear fit has been removed) after traces with significant ripples are discarded ($\sim$ 5%). The residuals are of order 0.015 dB in magnitude and 0.1° in phase, and since they are not dominated by noise (especially the black lines, which correspond to the average of all good traces), they represent systematic effects that the calibration procedure does not calibrate away.

Figure 9

The next slide (Figure 9) shows the reflection coefficient of an open-ended cable, $\sim$ 7-meters long, measured at the input of the receiver which at this point was underground, since the pit box was covered with the base plate. This measurement was done on day 298, lasted $\sim$ 3 hours, and was conducted to complement measurements of cable spectra.

The figure shows the average of the first and last 25 traces (out of $\sim$ 190), in order to improve the signal-to-noise ratio and identify significant changes in the cable reflection due to, for example, changes in ambient temperature. The differences between these two cases are small, within 0.015 dB and 0.15°.

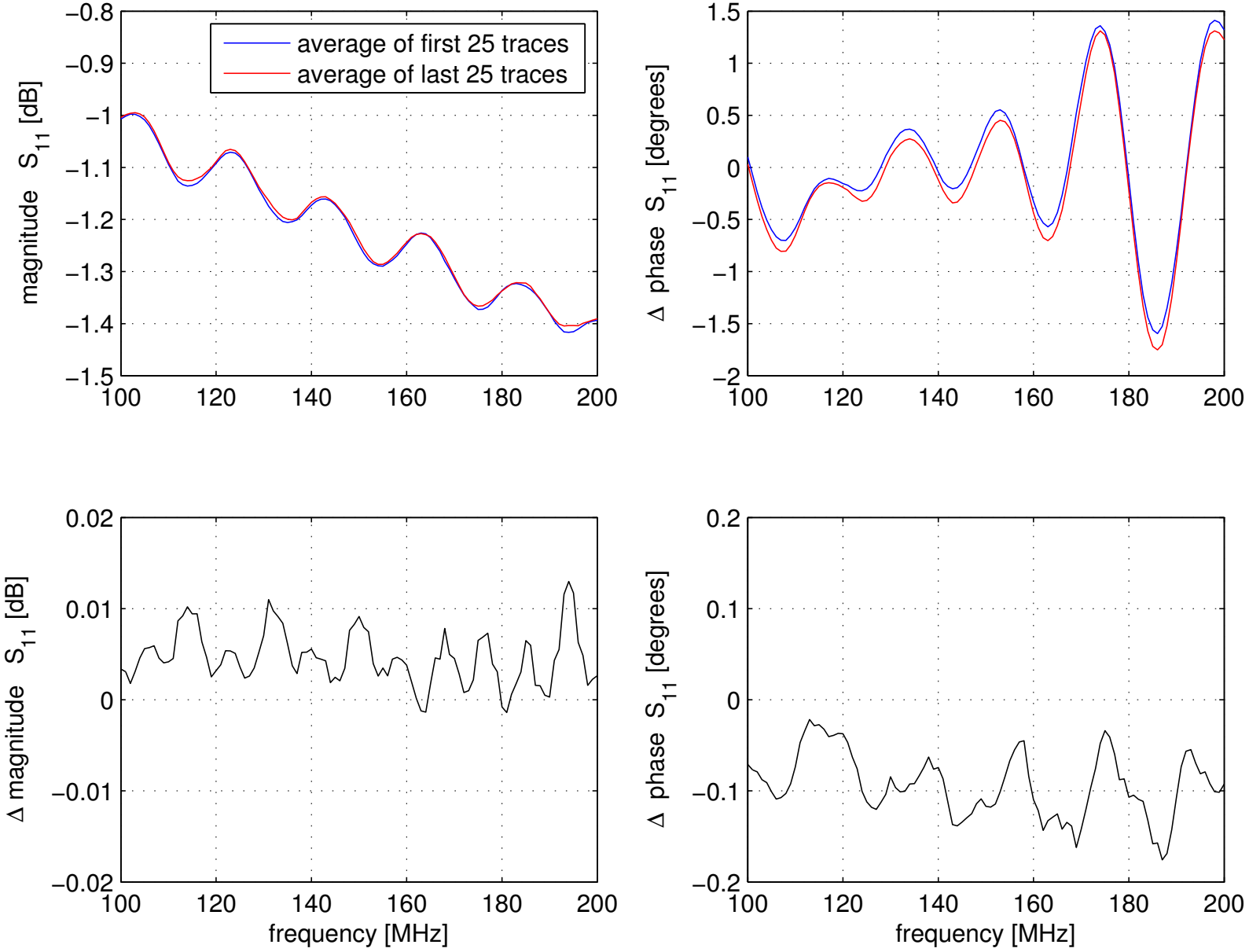

Figure: (9) Reflection of open cable measured at the input of the receiver, at the MRO, on day 298. The measurement lasted $\sim$ 3 hours. The average of the first 25 traces differs only by 0.015 dB and 0.15° from the average of the last 25 traces, as shown in the bottom panels. A linear fit has been removed from the phases, in the upper right panel.

Figures 10 and 11

On day 295, EDGES came online, and on day 296 its reflection was measured; after a short measurement of a few cycles, a longer measurement ($\sim$ 1-hour long) was conducted. Around the middle of the 1-hour measurement, the reflection changed significantly. The conditions during this measurement were:

1. The metal base plate was not bolted to the rest of the ground plane and would have only made contact at a few places.
2. The horizon shield was not bolted to the ground plane and may have been touching the balun.
3. The bottom tuning cross-bar was still in place.
4. The capacitance spacers at the edges of the dipoles were rotated at arbitrary angles.
5. The antenna had not been tuned by adjusting the upper cross-bar and tweaking the top-cap.

The change in antenna behavior could be explained by 1) or 2). Figures 10 and 11 show its response and the change it suffered. As expected, Figure 10 shows that the overall response was not optimal. Neither state (blue and red traces) is very good, and both present strange bumps in the region 160-180 MHz. At some point it was assumed that those bumps were the result of isolated problems with calibration (similar to those presented in Figure 6), but when all the traces are seen simultaneously it is clear that this response, and the sudden jump, represented the actual behavior of the antenna and not calibration abnormalities.

Figure 11 shows the differences of the reflection coefficient with respect to the average of traces belonging to the first state. As it can be seen, the jump that occurred between traces 24 and 25 produced changes of order $\pm$0.2 dB in magnitude and +2°/-1° in phase.

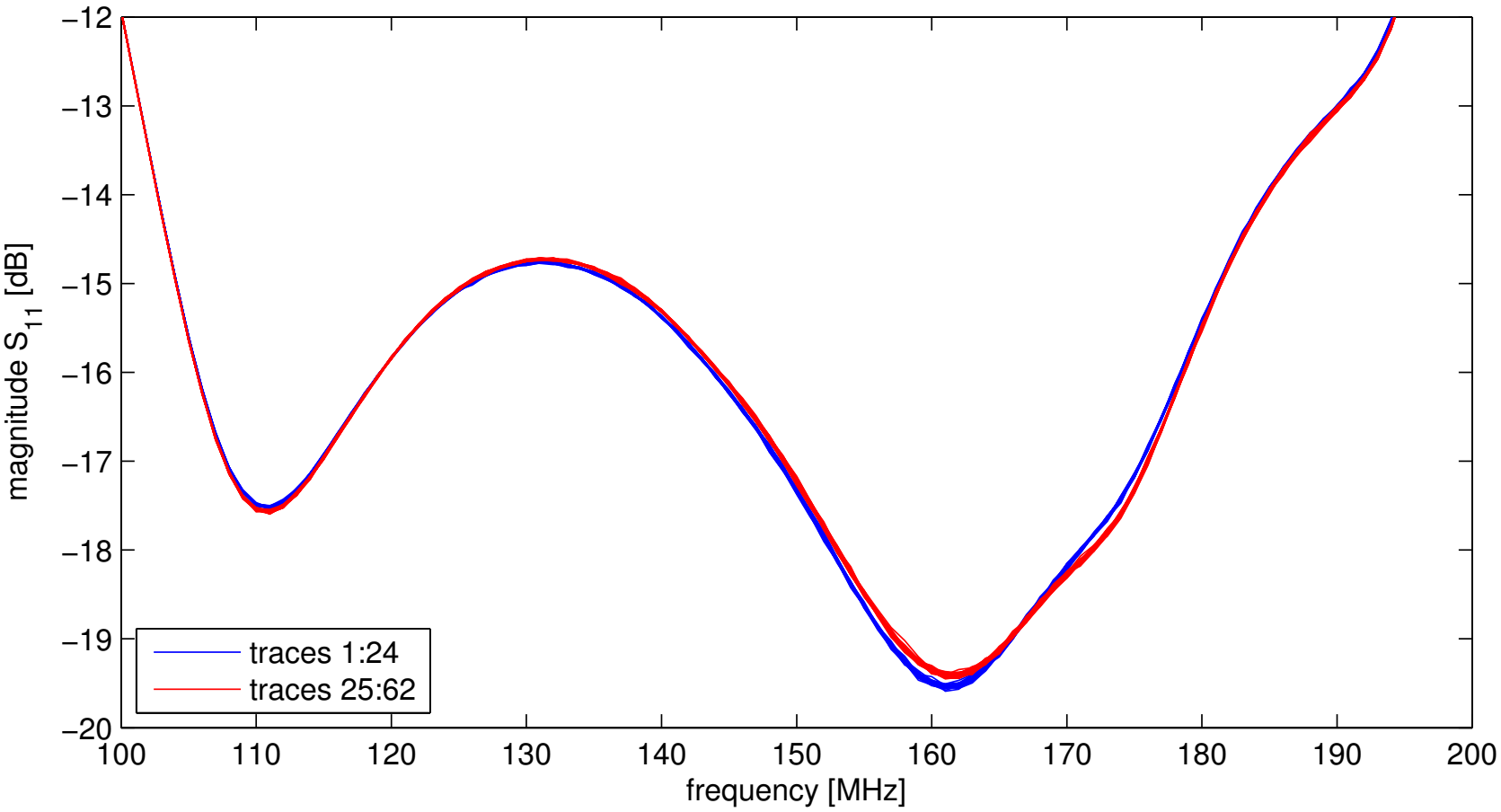

Figure: (10) Magnitude of the antenna reflection coefficient measured for about 1 hour on day 296. Blue and red colors are used to evidence a sudden change in the response of the antenna between traces 24 and 25.

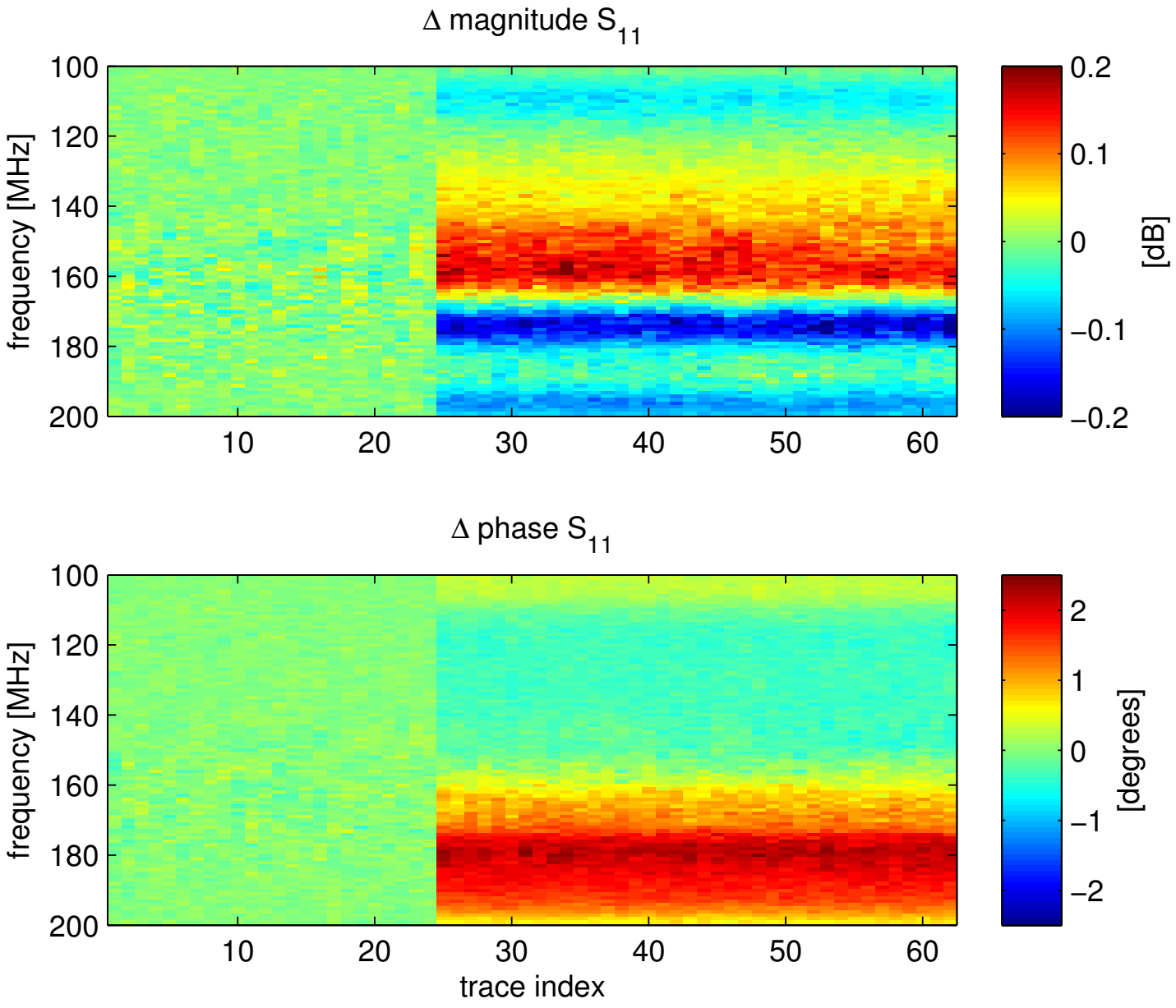

Figure: (11) This figure presents the changes of antenna reflection during the 1-hour measurement of day 296, relative to the average of the first 24 traces. The jump that occurred between trace 24 and 25 produced changes of order ± 0.2 dB in magnitude and $+2^\circ/-1^\circ$ in phase.

Figures 12 through 17

The final tuning of the antenna was conducted on days 300 and 301, before Judd and Cassie left the site. The results for each day are presented in Figure 12. The result for day 2 (300) is the one that should ideally represent the response of the antenna since then. For this day, the best reflection (lowest, in a wideband sense) was found with the tuner set so the bottom of the upper bar is at 31.9 cm from the base plate, and the quartz rotated so that there is maximum capacitance. Other details include:

1. No lower cross-bar.
2. The shield is attached to the baseplate.
3. The topcap is in its standard position

Pictures 13 through 17 give an idea of the state of the antenna at the site just before Judd and Cassie left the site.

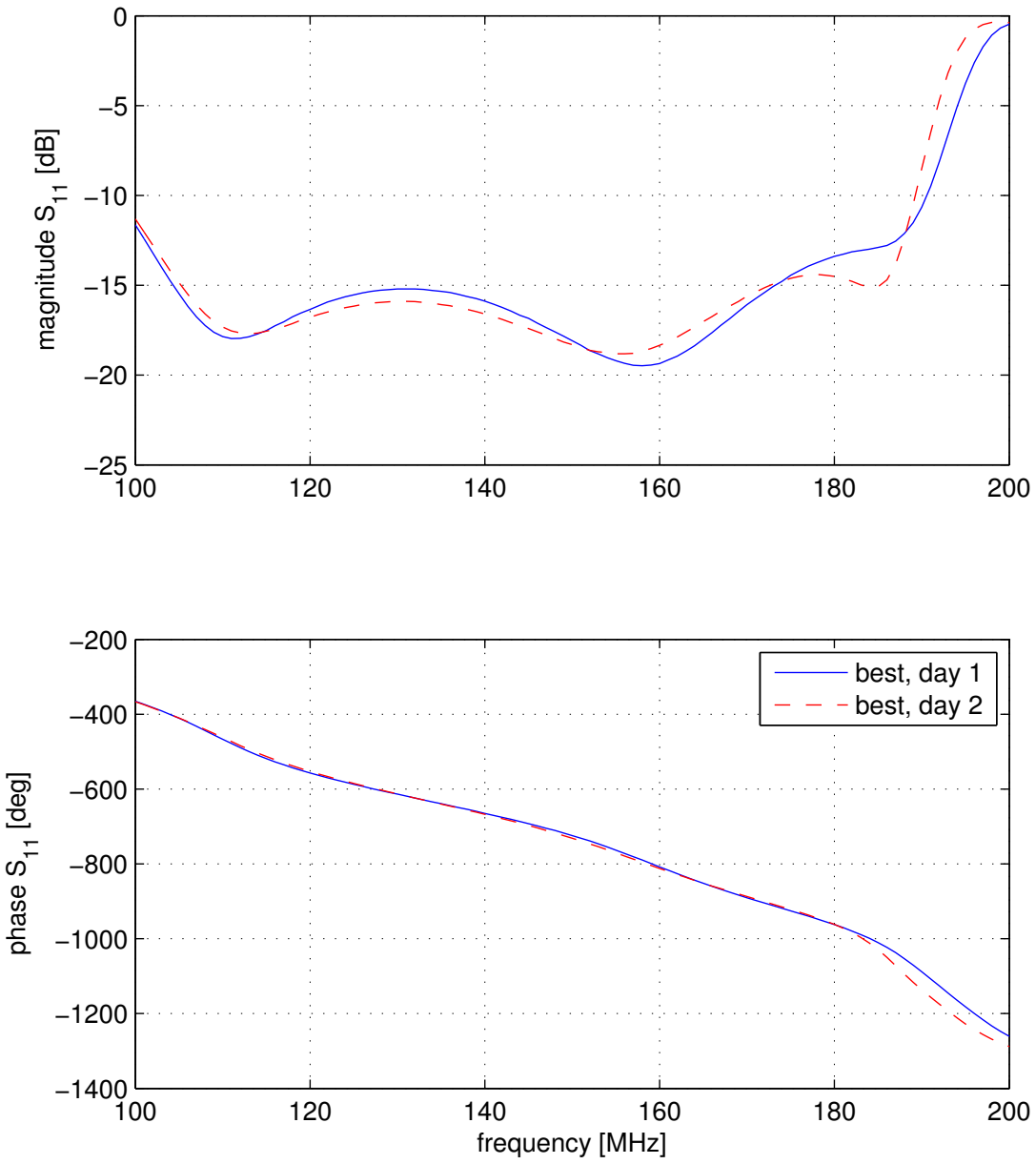

Figure: (12) Best antenna responses obtained during the tuning of days 1 (300) and 2 (301). The response of day 2 is the one expected to represent the antenna since then.

Figure: (13) Overall view of the antenna and ground plane, relative to the hut and ASKAP antenna.

Figure: (14) Bottom view of the antenna.

Figure: (15) Zoom in on the top plate.

Figure: (16) Zoom in on the tuner capacitor.

Figure: (17) Zoom in on one edge capacitor.